Clinical Neuroradiology (2023) 33:293–306
https://doi.org/10.1007/s00062-022-01231-5

REVIEW ARTICLE

Cerebral Superficial Siderosis

Etiology, Neuroradiological Features and Clinical Findings

Stefan Weidauer[1] · Elisabeth Neuhaus[1] · Elke Hattingen[1]

Received: 25 May 2022 / Accepted: 11 October 2022 / Published online: 28 November 2022

Abstract
Superficial siderosis (SS) of the central nervous system constitutes linear hemosiderin deposits in the leptomeninges and the superficial layers of the cerebrum and the spinal cord. Infratentorial (i) SS is likely due to recurrent or continuous slight bleeding into the subarachnoid space. It is assumed that spinal dural pathologies often resulting in cerebrospinal fluid (CSF) leakage is the most important etiological group which causes iSS and detailed neuroradiological assessment of the spinal compartment is necessary. Further etiologies are neurosurgical interventions, trauma and arteriovenous malformations. Typical neurological manifestations of this classical type of iSS are slowly progressive sensorineural hearing impairment and cerebellar symptoms, such as ataxia, kinetic tremor, nystagmus and dysarthria. Beside iSS, a different type of SS restricted to the supratentorial compartment can be differentiated, i.e. cortical (c) SS, especially in older people often due to cerebral amyloid angiopathy (CAA). Clinical presentation of cSS includes transient focal neurological episodes or "amyloid spells". In addition, spontaneous and amyloid beta immunotherapy-associated CAA-related inflammation may cause cSS, which is included in the hemorrhagic subgroup of amyloid-related imaging abnormalities (ARIA). Because a definitive diagnosis requires a brain biopsy, knowledge of neuroimaging features and clinical findings in CAA-related inflammation is essential. This review provides neuroradiological hallmarks of the two groups of SS and give an overview of neurological symptoms and differential diagnostic considerations.

Keywords Superficial siderosis · Infratentorial · Cortical · Amyloid related imaging abnormalities · Cerebral amyloid angiopathy

Introduction

Superficial siderosis (SS) of the central nervous system (CNS) constitutes linear hemosiderin in the leptomeninges and the superficial layers of the cerebral and cerebellar cortices, the brainstem and the spinal cord [1–3]. Infratentorial (i) SS was first described by Hamill in 1908 as a "case of melanosis of the brain, cord and meninges", particularly involving the infratentorial structures in the posterior fossa and the spinal cord [4]. An iSS is often caused by chronic intermittent or continuous slight bleeding into the subarachnoid space [5–8]. The most common etiology is spinal dural abnormalities, often dural tears (classical or type 1 iSS). In addition, CNS tumors, arteriovenous malformations (AVM), head or spinal trauma and craniospinal surgery can also cause iSS [1, 2, 8–15]. Neuroimaging typically shows symmetrical involvement of posterior fossa structures. Less commonly, iSS may be due to an isolated causative subarachnoid hemorrhage (SAH) event, e.g. aneurysm rupture, AVM or CNS trauma. In this type 2 iSS (secondary iSS) magnetic resonance imaging (MRI) appearance of SS is likely asymmetric and predominantly focused around the bleeding site (see Fig. 1). In contrast to classical iSS, progressive cerebellar ataxia and impaired hearing are lacking on neurological examination [8, 15].

Besides iSS, a different type of so-called localized SS, i.e. cortical (c) SS can be differentiated, which is restricted to the supratentorial compartment (see Fig. 1; [15–25]). A cSS is characterized by asymmetric and focal areas of hemosiderin depositions in the cortical sulci, based on var-

✉ Stefan Weidauer
weidauer@em.uni-frankfurt.de

[1] Institute of Neuroradiology (1), Goethe University, Schleusenweg 2–16, 60528 Frankfurt am Main, Germany

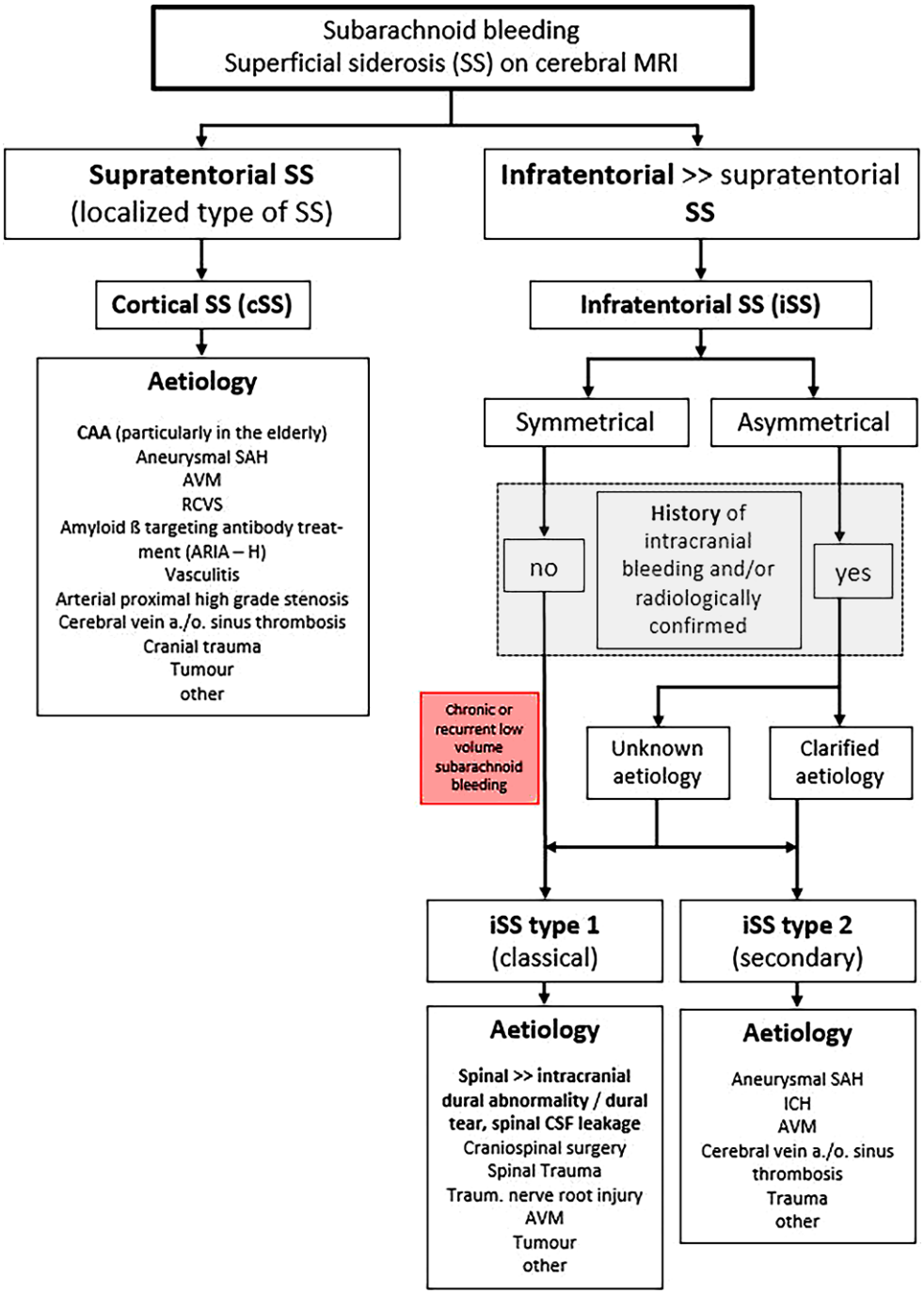

Fig. 1 Algorithm of different types of superficial siderosis (SS) and the corresponding assumed etiologies. *ARIA—H*: amyloid-related imaging abnormalities, hemorrhagic type, *AVM* arteriovenous malformation, *CAA* cerebral amyloid angiopathy, *CSF* cerebrospinal fluid, *ICH* intracerebral hemorrhage, *RCVS* reversible cerebral vasoconstriction syndrome, *SAH* subarachnoid hemorrhage

ious etiologies other than in iSS [2, 9, 15–25]. Especially in older patients cSS is often due to cerebral amyloid angiopathy (CAA) [2, 18, 19]; however, not only the neuroradiological findings and the causes but also the clinical symptoms clearly differ between the two types of iSS [2, 9, 10, 15, 21]. This review deals with the characteristic neuroimaging features in iSS and cSS and also gives an overview of clinical symptoms and differential diagnostic considerations.

Infratentorial Superficial Siderosis (iSS)

From a neuropathological point of view the hemosiderin deposits and especially the neurotoxic iron in the leptomeninges and the subpial structures lead to demyelination, axonal loss and subsequent atrophy [1, 3, 5, 6]. There is a sharp delineation of hemosiderin deposits in the cranial nerves and the spinal nerve roots directly at the transition zone of central glial cells and peripheral Schwann cells [1, 3, 5, 6, 13]. Therefore, the olfactory nerve and the vestibu-

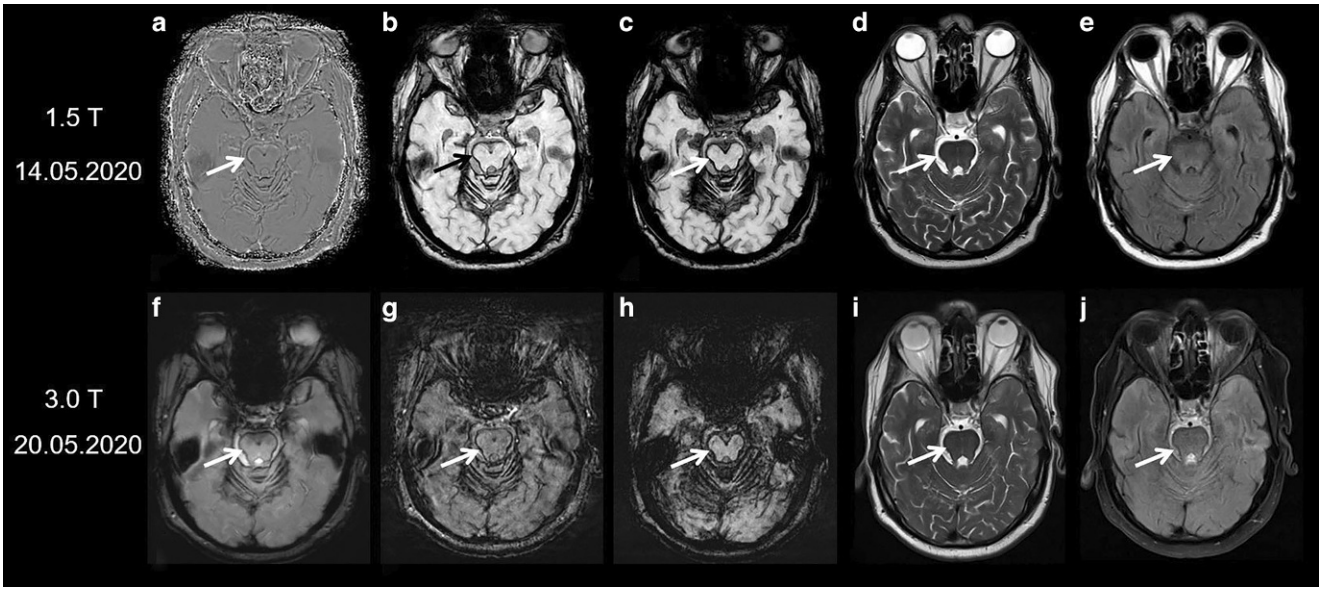

Fig. 2 Diagnostic value of different MRI sequences in the detection of superficial siderosis (SS). A 61-year-old man with SS due to ongoing hemorrhage from a melanoma metastasis in the right frontal cortex. In T2*-GRE (**f**) and susceptibility-weighted imaging (SWI) (**b**,**g**), SS is revealed by dark rims on the surface of affected structures, e.g., the mesencephalon (*arrow*), with SWI being more sensitive. Minimum intensity projections (mIPs) of SW images (**c**,**h**) further enhance the conspicuousness of SS. In addition, filtered phase image of SWI (**a**) can be used to distinguish paramagnetic (hemorrhage/iron, *dark* here) from diamagnetic substances (calcification, *bright* here), as they have opposite signal intensities. In general, susceptibility effects are more pronounced on images acquired at 3 T (**f**–**j**) than on images acquired at 1.5 T (**a**–**e**). Whereas at 3 T a hypointense rim around the mesencephalon is seen in T2WI and fluid attenuated inversion recovery (FLAIR) images (**i**,**j**, *arrow*), SS is almost undetectable at 1.5 T in T2WI and FLAIR (**d**,**e**, *arrow*). **a–e** 1.5 T (Achieva dStream, Philips); **a**–**c** SWI, TR/α 52 ms/20°, 4 echoes TE1 = 12 ms, ΔTE = 11 ms; **d** T2, TR/TE/α = 5762 ms/110 ms/90°; **e** FLAIR, TR/TE/TI/α = 11000 ms/140 ms/2800 ms/90°; **f**–**j** 3 T (Skyra fit, Siemens); **f** T_2*-GRE, TR/TE/α = 631 ms/20 ms/20°; **g**, **h** SWI, TR/TE/α = 27 ms/20 ms/15°; **i** T2, TR/TE/α = 4980 ms/92 ms/150°, **j** FLAIR: TR/TE/TI/α = 8500 ms/81 ms/2440 ms/150°. *TR* repetition time, *TE* echo time, *TI* inversion time, *α* flip angle

locochlear nerve are preferentially involved, because both are pure glial nerves with close contact to the cerebrospinal fluid (CSF). Although the optic nerve represents the glial type, clinical signs of involvement are rare, possibly due to the shorter course through the subarachnoid space [7].

For many years a definitive diagnosis of SS could be established only by biopsy or post-mortem; however, due to the iron sensitive T2* gradient recalled echo (GRE) sequences or the more sensitive susceptibility weighted imaging (SWI) especially at higher field strength, SS exhibits characteristic imaging features with signal loss, i.e. dark rims on the surface of the affected structures [2, 18, 26–31]. The paramagnetic blood breakdown products, also including hemosiderin as a stable final product, cause local magnetic field inhomogeneity [2, 30, 31]. The radiological appearances of SS with different sequences and field strengths are illustrated in Fig. 2.

The most common etiology is spinal dural disease, often coming along with ventral dural tears, less commonly intracranial dural abnormalities inducing classical type of iSS (type 1) (see Figs. 3 and 4). Dural tears may be caused by at times calcified disc herniation and occasionally spiculated osteophytes, often associated with a ventrally accentuated epidural fluid collection due to CSF leakage [10–12, 14, 15]. Dural ventral tears are preferentially located in the upper thoracic spinal levels [8, 14, 15]. Further pathologies are intrinsic dural diseases caused by connective tissue abnormalities, spinal CSF venous fistula or nerve root diverticula, traumatic nerve root avulsion (see Fig. 5) and postoperative pseudo-meningoceles [8, 14, 15, 32]. Spontaneous intracranial hypotension (SIH) due to CSF leakage with similar intraspinal epidural fluid collection is associated with leptomeningeal hemosiderosis on MRI in 5–10% of patients [14, 33, 34]. Other less common etiologies for classical iSS are neurosurgical craniospinal interventions, trauma, cranial or spinal tumors and AVM [1, 8, 15]. Chronic ongoing or repetitive low-volume bleeding in the subarachnoid space can occur before the diagnostic conformation of a CNS tumor (see Fig. 2; [11]) or may be due to postoperative residual tumor tissue or a postsurgical cavity. There is evidence that AVMs found in the diagnostic work-up of SS are often incidental [8].

In type 2 iSS (secondary iSS) [5–13, 15] evidence of a causative often single SAH or parenchymal bleeding is radiologically present; however, in contrast to classical iSS MRI may disclose asymmetric iSS predominantly focused in the neighborhood of the bleeding site [8, 15]. It is worth noting that parenchymal bleeding may be caused by a ve-

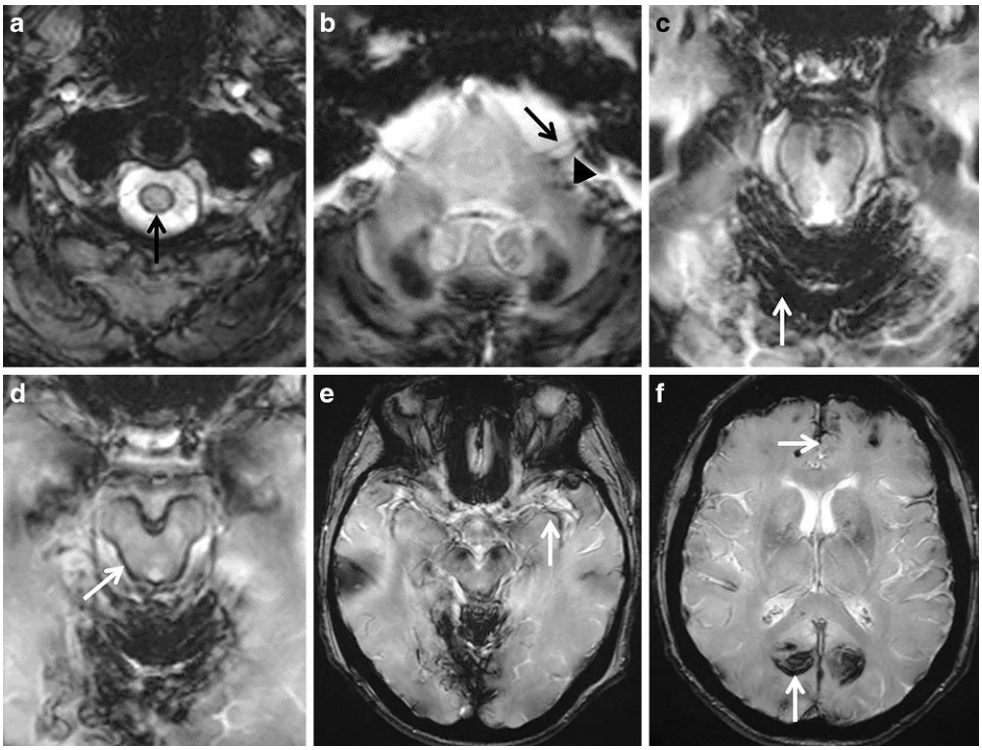

Fig. 3 Classical infratentorial superficial siderosis (iSS) in a 77-year-old woman with progressive hearing loss, gait ataxia, visual disturbances and optical hallucinations over 6 months. Axial T2*-GRE (**a**–**f**) showing SS of the upper cervical spinal cord (**a**, *arrow*), the VIII cranial nerve but sparing the VII cranial nerve (**b**: a*rrowhead*, *arrow*), the cerebellum and mesencephalon (**c**,**d**: *arrow*), the medial Sylvian fissure (**e**, *arrow*) and of the medial occipital lobes (**f**, *arrow*)

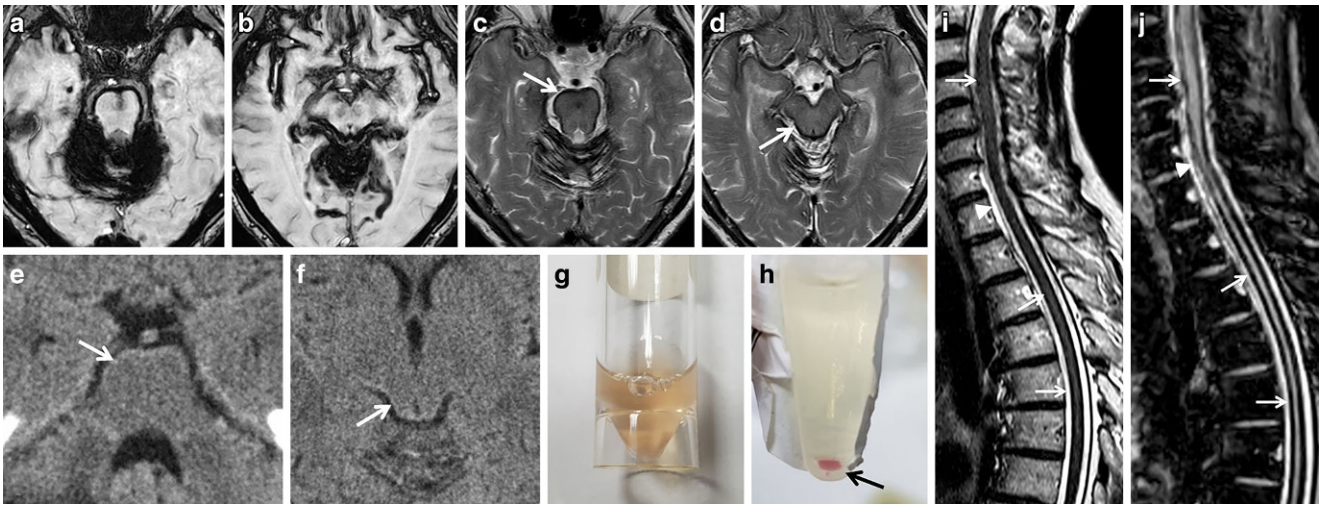

Fig. 4 A 73-year-old woman suffering from recurrent severe headache attacks due to ventral dural defect at the level of the second thoracic vertebra with spontaneous intracranial hypotension and recurrent subarachnoid bleeding over more than 10 years. Axial susceptibility-weighted imaging (SWI) (**a**,**b**) and axial T2-weighted images (WI) (**c**,**d**; *arrow*) showing extensive superficial siderosis (SS) especially infratentorial; **e**, **f** CT disclosing slight hyperdense pontine and mesencephalic surface (*arrow*). Cerebrospinal fluid (CSF) analysis demonstrating auburn liquor (**g**); **h** xanthochrome supernatant and sedimentation of erythrocytes after centrifugation (**h**, *arrow*). **i**,**j** (SWI sag.) Extensive spinal SS (*arrows*) and ventral epidural fluid collection at the upper thoracic level (*arrowheads*)

nous outflow disorder. In rare cases venous thrombosis can occur as a result of decreased intracranial pressure in so far undetected spinal dural CSF leakage [10, 12]. Therefore, it seems recommendable that the etiology of the bleeding event has to be clarified before the assignment to type 1 or 2 iSS is made (see Fig. 1).

Typical neurological manifestations of classical iSS (type 1) are slowly progressive sensorineural hearing impairment and cerebellar symptoms, such as ataxia, kinetic tremor, nystagmus and dysarthria (see Figs. 3 and 4; [7–9, 13]). Preferential affection of the cerebellar vermis results in severe ataxic gait disturbance up to inability to stand and walk [8]. In addition, spinal cord symptoms may occur,

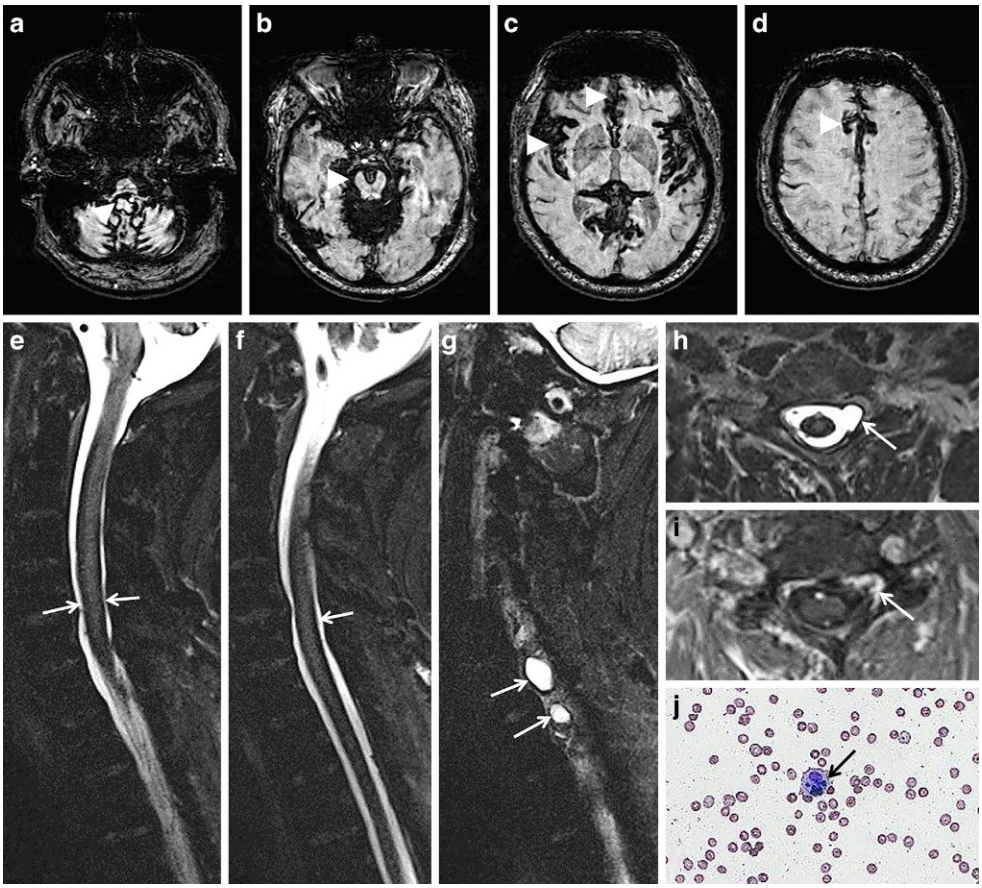

Fig. 5 Classical superficial siderosis (SS) in a 59-year-old man suffering from progressive gait ataxia within 6 months and traumatic nerve root injury C7 and C8 30 years ago. **a**–**d** Axial susceptibility-weighted imaging (SWI) showing SS with pial signal loss (*arrowheads*) especially in the posterior fossa (**a**,**b**) and partially supratentorial (**c**,**d**: *arrowheads*). **e**–**j** SS also of the spinal cord (**e**,**f**: T2*-weighted images [WI] sag.; *arrows*); enlarged empty nerve root pouches C7 and C8 left (**g**,**h**: T2* WI sag. and ax. *arrows*) with inhomogeneous contrast enhancement (**i**, post contrast T1 WI ax. *arrow*); **j** cerebrospinal fluid (CSF) analysis exhibits silent chronic subarachnoid bleeding with erythrocytes and siderophages (*arrow*; magnification: 200x)

especially corticospinal tract signs with spasticity, rarely also anterior horn signs (see Figs. 4 and 5; [6, 8, 12]). In contrast, in patients suffering from iSS type 2 these neurological symptoms are lacking [8, 15]. Contrariwise, predominately focal neurological deficits are often present depending on the localization and etiology of the pathologic process.

Patients suffering from SIH as sequelae of spinal dural CSF leakage often show orthostatic headache, dizziness and auditory disturbance, nausea and vomiting. Impressive amnestic hint is the statement "the day it all began" [10, 12, 14, 34]. Characteristic focal neurological symptoms are cranial nerve palsies, especially abducens nerve failure [14, 34]. Brain sagging results in consecutive mechanical stress of the abducens nerve due to the fixation within Dorello's canal when entering the clivus [34].

Beside MRI with thin slices, e.g. constructive interference in steady-state (CISS) and 3D T2 sampling perfection with application optimized contrasts using different flip angle evolutions (SPACE) [35], myelographic computed tomography (CT) and especially if indicated dynamic subtraction myelography are necessary to identify the circumscribed dural defect in classical iSS (see Fig. 1; [14, 36–38]). Overall, in more than 80% of patients with iSS a potentially causal spinal or cranial dural abnormality can be identified [8, 10, 15, 35]. An additional supportive therapeutic option in iSS is the administration of iron chelates [39].

Cortical Superficial Siderosis (cSS)

A cSS is a sequela of a previous acute cortical (c; or convexity) SAH with focal hyperdense sulcus on CT and hyperintense sulcal signal changes on fluid attenuated inversion recovery (FLAIR) images (see Fig. 6; [2, 16–19]). Terminology also includes subarachnoid hemosiderosis, sulcal siderosis and superficial cortical siderosis [2]. There is a further differentiation between local cSS involving 1–3 sulci and disseminated cSS affecting at least 4 sulci [40]. Whereas in the acute or subacute stage T2* WI and SWI show often homogeneous signal loss, in the chronic stage bilinear track-like appearance is typical (see Fig. 6; [2, 18]). Especially in older patients cSS is often due to cerebral amyloid angiopathy (CAA) (see Fig. 7). Further etiologies of cSS are aneurysm related SAH, AVM, reversible cerebral vasoconstriction syndrome (RCVS), vasculitis, arterial proximal high-grade stenosis, cerebral vein and/or sinus thrombosis, cranial trauma and also amyloid beta targeting antibody treatment (see Fig. 1; [8, 15, 41–49]).

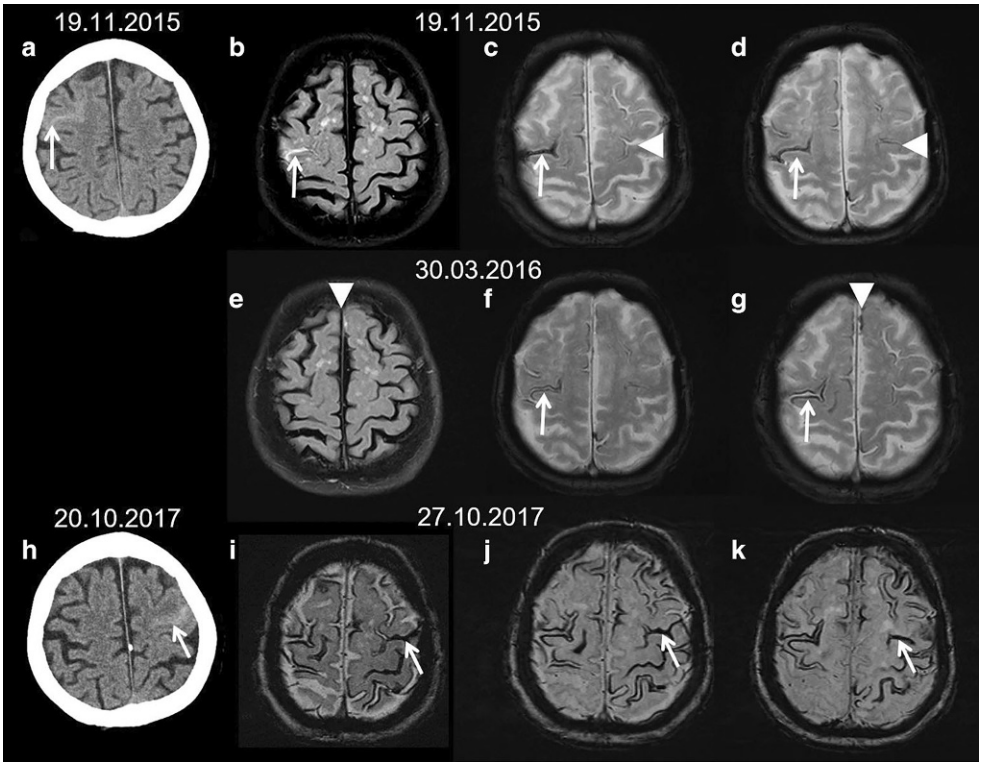

Fig. 6 A 74-year-old woman suffering from recurrent cortical subarachnoid hemorrhage (cSAH) in cerebral amyloid angiopathy (CAA). **a**–**d** First cSAH frontal right (**a**: CT ax., *arrow*) with sulcal hyperintense signal changes on fluid attenuated inversion recovery (FLAIR) images (**b**, *arrow*) and sulcal signal loss on T2*WI (**c**,**d**: *arrow*); additional cortical superficial siderosis (cSS) left (**c**,**d**: *arrowhead*); **e**–**g** second cSAH paramedian frontal left (**e**: FLAIR ax.; **g**: T2*WI ax.; *arrowhead*); note characteristic bilinear trackline appearance of cSS in the chronic stage (**f**,**g**: T2*WI, *arrow*); **h**–**k** third cSAH frontodorsal left (**h**: CT ax., *arrow*) with signal loss on SWI (**i**–**k**, *arrow*) and progressive cSS bilaterally

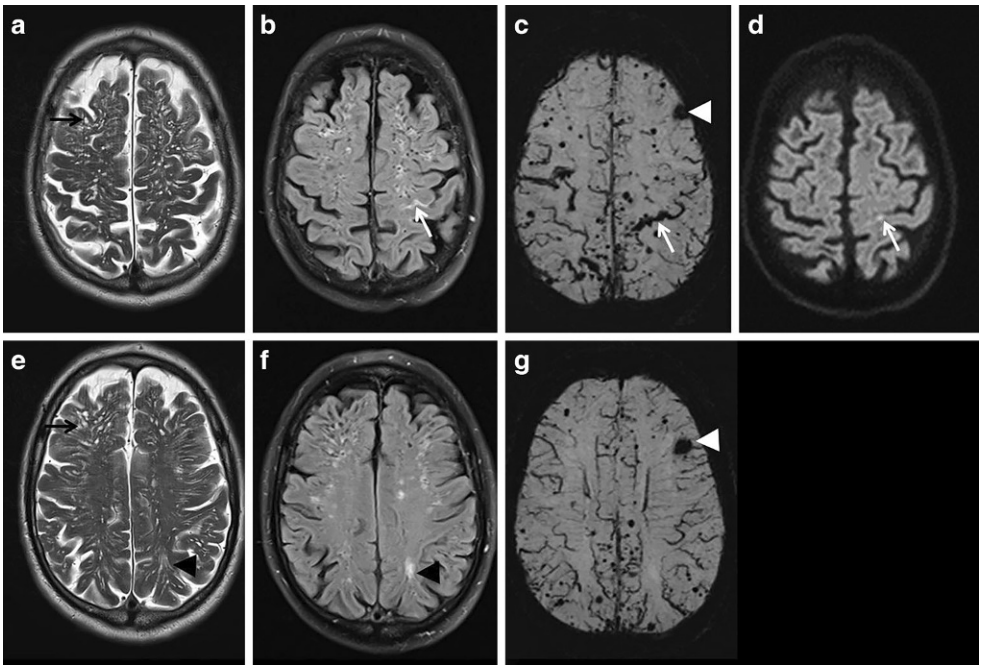

Fig. 7 A 72-year-old man with beginning dementia suffering from temporary hemiparesis right and aphasia due to cerebral amyloid angiopathy (CAA). Acute cortical subarachnoid hemorrhage (cSAH); **b** fluid attenuated inversion recovery [FLAIR ax.; **c** susceptibility-weighted imaging (SWI) ax.; **d** diffusion-weighted imaging (DWI) ax., b = 1000 s/mm^2, *arrow*. Enlarged perivascular spaces (PVS) (**a**,**e**: T2WI ax.; *arrow*), focal small gliosis (**b**,**f**: FLAIR ax.; *arrowhead*), multiple microbleeds (MB) and cortical superficial siderosis (cSS) (**c**,**g**: SWI ax.) beside residual atypical intracerebral bleeding frontal left (**c**,**g**: *arrowhead*)

Cerebral Amyloid Angiopathy (CAA)

CAA encompasses a genetic and biochemical inhomogeneous group of pathologies in which the reduced perivascular clearance of amyloid beta (Aß) from the interstitial fluid has a key role in the pathogenesis of CAA and Alzheimer's disease (AD) [50–55]. Beside an impairment of the intramural periarterial drainage (IPAD) an insufficient perivascular transport via the glymphatic system is also discussed [54–56]. In consequence, there are deposits especially in the small and medium sized arteries in the cortex and the leptomeninges with preference of the posterior lobar brain regions [54, 57–59]. Whereas capillary involvement is classified as CAA type 1, type 2 reflects CAA without deposits

in the capillaries [60–63]. Apolipoprotein (APO) E ε4 expression is a risk factor for CAA especially with capillary type 1 and APO E ε2 is associated with type 2 [60–63]. Aß-42 is less soluble and parenchymal fibrils are a likely consequence, while the more soluble Aß-40 preferentially accumulates in the vessel walls [60, 64–66]. Arterial pulsation and vasomotion generated by the smooth muscle cells enable and facilitate interstitial drainage [53–55]; however, vascular Aß deposits interfere with these mechanisms due to reduced vessel wall volubility, establishing a self-reinforcing cycle of reduced Aß clearance and widened perivascular spaces (see Fig. 7; [54, 60, 67, 68]).

Neuroradiological hallmarks of CAA are multiple cortical and subcortical lobar microbleeds (MB) [27, 60, 69]. In contrast, MB caused by lipohyalinosis, arteriosclerosis and fibrinoid necrosis of the small perforators related to aging and common vascular risk factors, i.e. arterial hypertension and diabetes, are located in the basal ganglia, thalamus, pons and the cerebellum [27, 70–77]. Consecutively, typical intracerebral hemorrhages (ICH) associated with hypertension appear in these regions, whereas CAA related atypical ICH are located in the cerebral lobes with high risk of recurrence (see Fig. 7; [69, 70, 78–81]). APO Eε2 is a risk factor for hemorrhagic CAA, whereas the APO Eε4 allele is a major risk factor for AD and CAA, the latter often with a severe clinical course [60, 64, 82–86]. In addition, CAA induce white matter hyperintensities with conflating appearance over time (see Fig. 7; [60, 73, 75, 77]). As a result of interaction between neurodegenerative and cerebrovascular processes in cerebral Aß deposition, subcortical MB preferentially parieto-occipital not only occur in CAA but also in AD [60, 73, 77, 87–92].

Although cSS includes several etiologies of cSAH (see Fig. 1; [2, 8, 15, 41–49]), especially in older individuals cSS is an important neuroimaging feature in CAA [2, 17, 19, 25, 60, 69, 93]. In the seminal publication by Linn et al. in 2010 [19] cSS was detected in 60.5% of patients suffering from CAA, mean age 70 ± 6.4 years. In contrast none of the controls showed cSS. Whereas the classic Boston criteria had a sensitivity of nearly 90% for CAA related hemorrhage, inclusion of cSS raised the sensitivity up to 94.7% [19]. In consequence, focal or disseminated cSS beside singular lobar cortical or subcortical hemorrhage were included as imaging criteria for probable CAA in the modified Boston criteria (see Fig. 6; [69, 70]).

Typical neurological presentation of cSS in CAA includes transient focal neurological episodes or "amyloid spells" [9, 83, 94–96]. These represent stereotypical positive or negative neurological symptoms depending on the localization of the initial cSAH and the developing cSS. For example, involvement of the central sulcus with affection of the precentral or postcentral gyrus will cause contralateral propagating sensory or motor symptoms. From a pathophysiological point of view cortical spreading depolarization is discussed [83, 94, 96, 97]. Knowledge of this clinical feature in CAA associated with cSS is crucial. Focal epileptic seizures, e.g. sensory or motor Jacksonian seizures or ischemia, e.g. transient ischemic attacks, may mimic cSS related symptoms with possible wrong therapeutic consequences of antiepileptic or antithrombotic medication [75, 77, 95, 96]. Further differential diagnoses include focal vasospasms, RCVS and cortical venous thrombosis (see Fig. 8; [15, 41, 42, 73]). Neuroradiological hints and clinical symptoms to differentiate imaging mimics of cSS from "true" cSS are summarized in Table 1 [30, 31, 41, 42, 98–102].

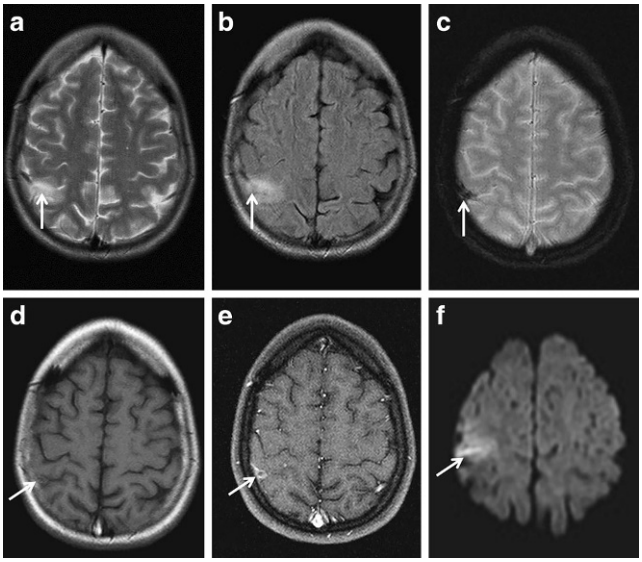

Fig. 8 Cortical vein thrombosis as a possible mimic of cortical superficial siderosis (cSS) in a 27-year-old woman with right-sided headache and sensory Jacksonian seizures. MRI demonstrating cortical hyperintense lesion postcentral parietal right (**a**: T2 WI ax.; **b** fluid attenuated inversion recovery [FLAIR] images ax.; *arrow*), signal loss and "blooming" of the central vein (**c**, T2*WI ax.; *arrow*) without cSS, circumscribed peripheral contrast enhancement (**d**,**e** T1 WI ax., post contrast T1 WI ax.; *arrow*) and restricted diffusion of the thrombus (**f**, diffusion-weighted imaging [DWI] ax., b = 1000 s/mm^2, *arrow*)

CAA Related Inflammation (CAA-ri)

CAA related inflammation (CAA-ri) is a disease subtype associated with autoantibodies against Aß deposits in the vessel walls of cortical and leptomeningeal small and medium sized arteries, arterioles and capillaries [103–106]. The vascular and perivascular inflammation cause vasogenic edema and sulcal effusions with hyperintense signal changes on T2 WI and FLAIR images, i.e. amyloid related imaging abnormalities-edema (ARIA-E) (see Fig. 9; [48, 49, 107, 108]). The hemorrhagic type (ARIA-H) shows cerebral MB and cSS [40, 41, 108]. Neurological presentation of CAA-ri is characterized by rapidly progressive cognitive decline with

Table 1 Mimics of cortical superficial siderosis

Disease	Differential diagnostic hints	
	Imaging features	Neurological symptoms
Cortical vein thrombosis	*MRI*	–
	Pronounced "blooming effect" (T2*WI, SWI)	Focal epileptic seizures (e.g. sensible or motor Jacksonian seizures)
	Tubular aspect (parallel to thrombosed vein)	Focal neurological deficits
	Facultative hyperintense signal (T2, FLAIR) of adjacent cortex	(Facultative progressive, prolonged onset)
	Facultative intravasal diffusion restriction	Facultative headache
	CT	–
	"Cord sign" (hyperdense vein sign)	–
	"Missing vein", filling defect (CTA)	
Cortical hemorrhagic transformation in cerebral infarcts	*MRI*	–
	Petechial or broad linear or serpiginous signal loss (T2*WI, SWI)	Apoplectiform onset of (focal) neurological deficits
	Often additional subcortical tissue damage	Focal (or secondary generalized) seizures
	Acute/subacute stage: diffusion restriction	Facultative headache
	Chronic stage: gliosis	
	CT	–
	Hyperintense cortical band	–
	Often hypointense additional cerebral infarct	
Laminar cortical necrosis (e.g. hypoxic injury, status epilepticus)	*MRI*	–
	T1WI: hyperintense cortical/bandlike signal	Focal neurological deficits
	T2*WI/SWI: hypointense cortical/bandlike signal	Seizures
	DWI: cortical/band-like diffusion restriction in the acute stage	Facultative impairment of consciousness
		Facultative disturbance of vigilance
		Different states of confusion
Sturge Weber syndrome	*MRI*	–
	T2*WI/SWI: hypointense signal/signal loss possibly cortical and linear	Phacomatosis (encephalotrigeminal angiomatosis)
	SWI phase: negative (differentiation between diamagnetic mineralization and paramagnetic hemosiderin)	Neuropsychological deficits
		Seizures
	CT	–
	Hyperdense possibly bandlike calcifications	–
Calcifying angiopathy/ mineralizing microangiopathy	*MRI*	–
	T2*WI/SWI: cortical bandlike, linear hypointense/signal loss, often symmetric	Slowly progressive focal neurological symptoms, e.g. visual disturbances
	SWI phase: negative	
	Especially occipital lobes	
	CT	–
	Bandlike hyperdense cortex, often symmetric	–
Cockayne syndrome	*MRI*	–
	T2*WI/SWI: hypointense signal/signal loss in the basal ganglia, less often in the dentate nucleus and cortex	Neurodegenerative disorder
	SWI phase: negative	Four clinical overlapping syndromes
	Myelination disorder (hypomyelination or demyelination)	Congenital cataract
	Major brain atrophy	Type 1 (classical type) begins in infancy, death occurs in first decades of life
	CT	–
	Calcification	–

CT Computed Tomography, *CTA* Computed tomography angiography, *FLAIR* Fluid attenuated inversion recovery, *MRI* Magnetic resonance imaging, *SWI* Susceptibility-weighted imaging, *T2*WI* T2*-weighted images

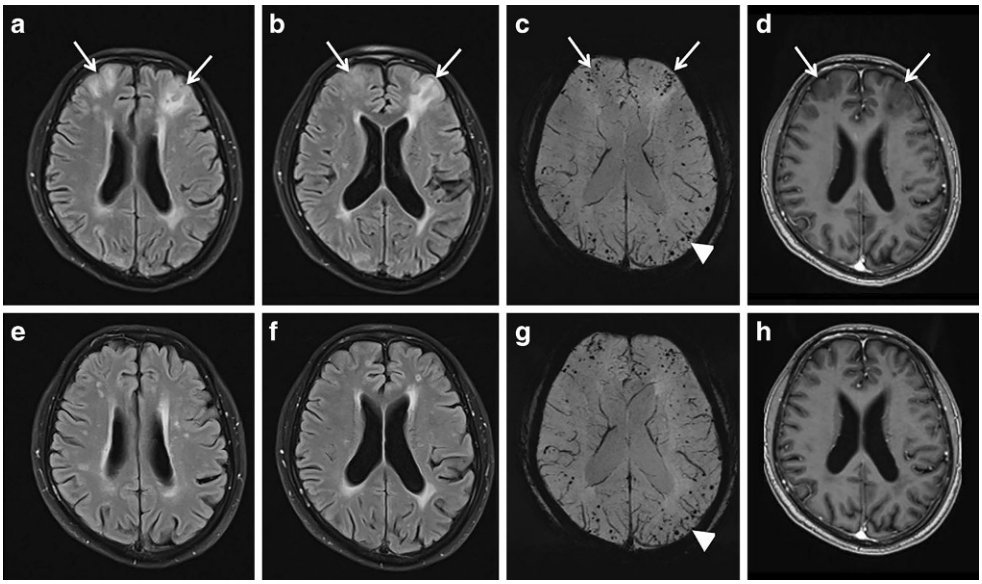

Fig. 9 CAA related inflammation (CAA-ri) in a 61-year-old man suffering from subacute psychosyndrome with disturbance of consciousness and executive disorders. **a**–**d** bifrontal left dominant hyperintense lesions with sulcal effusions (**a**,**b**: fluid attenuated inversion recovery [FLAIR] images ax.; *arrows*), accentuated microbleeds (MB) (**c**, susceptibility-weighted imaging [SWI] ax.; *arrows*) and hypointense signal conversion on postcontrast (pc) T1 WI (**d**, *arrows*) with enhancement; **e**–**h** follow-up MRI 13 months later after 3 bouts of high-dose methylprednisolone infusions, neurological examination was unremarkable. Completely resolved lesions frontal (**e**,**f**), unchanged cortical and subcortical MB (**c**,**g**; *arrowheads*)

impairment of consciousness, headache, seizures and variable focal neurological deficits depending on the localization of the autoimmune process [104, 109–111]. Diagnostic criteria differentiate between probable and possible CAA-ri [104]. In probable CAA-ri MRI discloses uni- or multifocal subcortical or deep white matter hyperintensities that are asymmetric and extend to the immediately subcortical white matter, and asymmetry is not due to past ICH [48, 104, 105, 110]. The patients are of age ≥ 40 years and neoplastic, infectious or other etiologies must be excluded. Because definitive diagnosis requires brain biopsy, knowledge of neuroradiological features in CAA-ri is essential [104, 110, 112]; however, from a histological point of view CAA-ri summarizes perivascular inflammation with histiocytes and also vessel wall inflammation with lymphocytes, and changeover to Aß related angiitis (ABRA) is not further differentiated [113–116].

There is evidence that intravenous (i.v.) high-dose corticosteroid pulse therapy with slow oral tapering is effective in spontaneous CAA-ri with neurological recovery in 84% within 1 year (see Fig. 8; [104, 110, 117, 118]); however, especially when i.v. corticosteroid therapy is stopped suddenly, in 34% recurrence within 24 months was observed. Focal brain atrophy is a likely consequence in nonresponders to anti-inflammatory treatment [104, 112].

Amyloid beta (Aß) Targeting Monoclonal Antibody Therapies

Different randomized clinical trials within the investigational use of monoclonal antibodies targeting Aß including aducanumab and bapineuzumab showed ARIA-E and ARIA-H. This suggests that immunotherapy related ARIA is an iatrogenic version of CAA-ri [40, 59, 81, 82, 108, 119, 120]. Due to increased parenchymal trafficking of Aß to the perivascular pathway during immunization with monoclonal antibodies the Aß overflow may lead to a disruption of smooth cells in the vessel wall [54, 60]. The extravasation of fluid with elevated protein content causes ARIA-E with edema and sulcal effusions, depending on the location of affected intraparenchymal and/or leptomeningeal vessels (Fig. 9; [40, 48, 60, 81, 82]). Whereas a single hyperintense lesion on FLAIR images smaller than 5 cm reflects mild severity, lesions > 5 and ≤ 10 cm are classified as moderate and lesions > 10 cm reflect severe ARIA-E [48]. Extravasation of blood cells causes ARIA-H, whereas up to 4 MB are considered as mild, 5–9 MB reflects moderate and ≥ 10 MB reflects severe ARIA-H [50]. In addition, also new areas of cSS (1, 2 or > 2) represent a mild, moderate or severe stage, respectively [40, 81]. The number of MB at baseline and the APO-Eε4 allele are risk factors for ARIA-E and ARIA-H. The risk of ARIA-E also depends on the antibody dosage and patients suffering from ARIA-E are at higher risk for additional ARIA-H [40, 108]. In the EMERGE and ENGAGE phase 3 randomized clinical trials

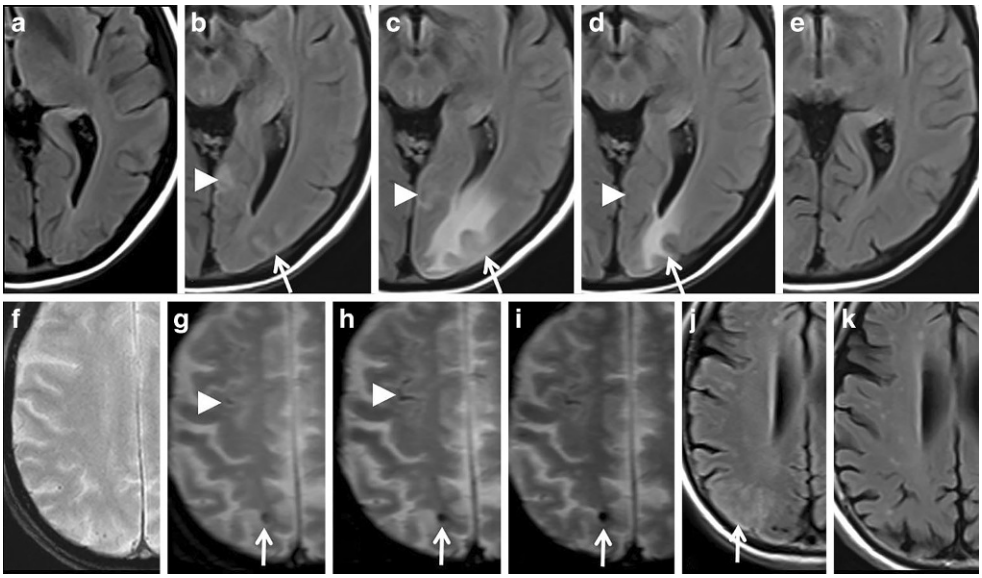

Fig. 10 Amyloid related imaging abnormalities (ARIA). **a**–**e** fluid attenuated inversion recovery [FLAIR] images ax. showing encephalopathic type of ARIA (ARIA—E) in a 54-year-old man treated with aducanumab, weeks 14 (**a**), 30 (**b**), 34 (**c**), 38 (**d**) 40 (**e**) after treatment initiation; sulcal effusions (**b**–**d**, *arrowhead*) and additional hyperintense lesion in the occipital lobe (**b**–**d**, *arrow*), which completely resolved at week 40. T2* WI ax. (**f**–**i**) and FLAIR ax. (**j**,**k**) demonstrating hemorrhagic type of ARIA (ARIA-H) and ARIA-E in a 68-year-old woman treated with aducanumab at baseline (**f**), weeks 14 (**g**), 18 (**h**,**j**), 20 (**i**) and 94 (**k**)

of aducanumab, ARIA-H associated cSS occurred in total in 14.7% of patients treated with a dose of 10 mg/kg and in APO-Eε4 carriers in 19.1% [108].

However, it is noteworthy that despite possible impressive imaging features the most common associated neurological symptom was headache [108]. Whereas ARIA-E was transient and resolved within 12–16 weeks after initial detection, ARIA-H tends to persist over time (see Fig. 10). It is hypothesized that vascular remodelling after Aß clearance might reduce further risk of ARIA over time [60, 108].

In conclusion, iSS is likely due to recurrent or continuous slight bleeding into the subarachnoid space, commonly due to spinal dural abnormalities, often dural tears (classical or type 1 iSS). Dural tears may be caused by at times calcified disc herniation and occasionally spiculated osteophytes, often associated with a ventrally accentuated epidural fluid collection due to CSF leakage. Further pathologies are intrinsic dural diseases caused by connective tissue abnormalities, CSF-venous fistula or nerve root diverticula, traumatic nerve root avulsion and postoperative pseudo-meningoceles. In consequence, detailed neuroradiological assessment of the spinal compartment is necessary, including MRI with thin slices, e.g. CISS and SPACE sequences, myelographic computed tomography (CT) and dynamic subtraction myelography. In SIH due to CSF leakage with similar intraspinal epidural fluid collection MRI concomitantly disclosed leptomeningeal hemosiderosis in 5–10% of patients.

In contrast, cSS especially in older patients is often due to CAA, encompassing a genetic and biochemical inhomogeneous group of pathologies in which the reduced perivascular clearance of Aß from the interstitial fluid has a key role in the pathogenesis. Typical clinical presentation of cSS in CAA includes transient focal neurological episodes or "amyloid spells". Knowledge of this neurological feature in CAA and associated cSS is essential to avoid clinical misinterpretation and subsequent wrong therapeutic interventions. In addition, CAA-ri may occur spontaneously or caused by Aß immunotherapy. In contrast to several grades of neuropsychological disturbances due to spontaneous CAA-ri, Aß immunotherapy associated ARIA-E and ARIA-H neurologically is often present with headache. In contrast, slowly progressive sensorineural hearing impairment and cerebellar symptoms up to severe ataxic gait disturbance reflect the neurological key symptoms in the classical type of iSS.

Funding Open Access funding enabled and organized by Projekt DEAL.

Conflict of interest S. Weidauer, E. Neuhaus and E. Hattingen declare that they have no competing interests.

References

1. Fearnley JM, Stevens JM, Rudge P. Superficial siderosis of the central nervous system. Brain. 1995;118:1051–66.
2. Charidimou A, Linn J, Vernooij MW, Opherk C, Akoudad S, Baron JC, Greenberg SM, Jäger HR, Werring DJ. Cortical superficial siderosis: detection and clinical significance in cerebral amyloid angiopathy and related conditions. Brain. 2015;138:2126–39.
3. Koeppen AH, Dentinger MP. Brain hemosiderin and superficial siderosis of the central nervous system. J Neuropathol Exp Neurol. 1988;47:249–70.
4. Hamill RC. Report of a case of melanosis of the brain, cord, and meninges. J Nerv Men Dis. 1908;35(9):594.
5. Koeppen AH, Dickson AC, Chu RC, Thach RE. The pathogenesis of superficial siderosis of the central nervous system. Ann Neurol. 1993;34:646–53.
6. Koeppen AH, Michael SC, Li D, Chen Z, Cusack MJ, Gibson WM, Petrocine SV, Qian J. The pathology of superficial siderosis of the central nervous system. Acta Neuropathol. 2008;116:371–82.
7. Kumar N, Cohen-Gadol AA, Wright RA, Miller GM, Piepgras DG, Ahlskog JE. Superficial siderosis. Neurology. 2006;66:1144–52.
8. Kumar N. Superficial siderosis: a clinical review. Ann Neurol. 2021;89:1068–79.
9. Kumar S, Goddeau RP Jr, Selim MH, Thomas A, Schlaug G, Alhazzani A, Searls DE, Caplan LR. Atraumatic convexal subarachnoid hemorrhage: clinical presentation, imaging patterns, and etiologies. Neurology. 2010;74:893–9.
10. Friedauer L, Rezny-Kasprzak B, Steinmetz H, du Mesnil de Rochemont R, Förch C. Spinal dural leaks in patients with infratentorial superficial siderosis of the central nervous system-Refinement of a diagnostic algorithm. Eur J Neurol. 2022;29:1136–44.
11. Friedauer L, Foerch C, Steinbach J, Hattingen E, Harter PN, Armbrust M, Urban H, Steidl E, Neuhaus E, von Brauchitsch S. The Acute Superficial Siderosis Syndrome – Clinical Entity, Imaging Findings, and Histopathology. Cerebellum. 2022. https://doi.org/10.1007/s12311-022-01387-3. Epub ahead of print.
12. Friedauer L, Schaller MA, Steinmetz H, du Mesnil de Rochemont R, Seifert V, Hattingen E, Foerch C. Superfizielle Siderosen des zentralen Nervensystems: Folge jahrzehntelang persistierender spinaler Duralecks [Superficial siderosis of the central nervous system: A consequence of spinal dural leaks persisting for decades]. Nervenarzt. 2019;90:1274–8.
13. Spengos K, Koutsis G, Tsivgoulis G, Panas M, Vemmos K, Vassilopoulos D. Superficial siderosis of the central nervous system. Case report and review of the literature. Nervenarzt. 2004;75:492–5.
14. Urbach H, Fung C, Dovi-Akue P, Lützen N, Beck J. Spontaneous intracranial hypotension—presentation, diagnosis and treatment. Dtsch Arztebl Int. 2020;117:480–7.
15. Wilson D, Chatterjee F, Farmer SF, Rudge P, McCarron MO, Cowley P, Werring DJ. Infratentorial superficial siderosis: Classification, diagnostic criteria, and rational investigation pathway. Ann Neurol. 2017;81:333–43.
16. Charidimou A, Boulouis G, Fotiadis P, Xiong L, Ayres AM, Schwab KM, Gurol ME, Rosand J, Greenberg SM, Viswanathan A. Acute convexity subarachnoid haemorrhage and cortical superficial siderosis in probable cerebral amyloid angiopathy without lobar haemorrhage. J Neurol Neurosurg Psychiatry. 2018;89:397–403.
17. Charidimou A, Jäger RH, Fox Z, Peeters A, Vandermeeren Y, Laloux P, Baron JC, Werring DJ. Prevalence and mechanisms of cortical superficial siderosis in cerebral amyloid angiopathy. Neurology. 2013;81:626–32.
18. Linn J, Herms J, Dichgans M, Brückmann H, Fesl G, Freilinger T, Wiesmann M. Subarachnoid hemosiderosis and superficial cortical hemosiderosis in cerebral amyloid angiopathy. AJNR Am J Neuroradiol. 2008;29:184–6.
19. Linn J, Halpin A, Demaerel P, Ruhland J, Giese AD, Dichgans M, van Buchem MA, Bruckmann H, Greenberg SM. Prevalence of superficial siderosis in patients with cerebral amyloid angiopathy. Neurology. 2010;74:1346–50.
20. Linn J, Wollenweber FA, Lummel N, Bochmann K, Pfefferkorn T, Gschwendtner A, Bruckmann H, Dichgans M, Opherk C. Superficial siderosis is a warning sign for future intracranial hemorrhage. J Neurol. 2013;260:176–81.
21. Viswanathan A, Greenberg SM. Cerebral amyloid angiopathy in the elderly. Ann Neurol. 2011;70:871–80.
22. Calviere L, Cuvinciuc V, Raposo N, Faury A, Cognard C, Larrue V, Viguier A, Bonneville F. Acute Convexity Subarachnoid Hemorrhage Related to Cerebral Amyloid Angiopathy: Clinico-radiological Features and Outcome. J Stroke Cerebrovasc Dis. 2016;25:1009–16.
23. Geraldes R, Sousa PR, Fonseca AC, Falcão F, Canhão P, Pinho e Melo T. Nontraumatic convexity subarachnoid hemorrhage: different etiologies and outcomes. J Stroke Cerebrovasc Dis. 2014;23:e23–30.
24. DeSimone C, Graff-Radford J, El-Harasis MA, Rabinstein AA, Asirvatham SJ, Holmes DR. Cerebral amyloid angiopathy—diagnosis, clinical implications, and management strategies in atrial fibrillation. J Am Coll Cardiol. 2017;70:1173–82.
25. Wollenweber FA, Opherk C, Zedde M, Catak C, Malik R, Duering M, Konieczny MJ, Pascarella R, Samões R, Correia M, Martí-Fàbregas J, Linn J, Dichgans M. Prognostic relevance of cortical superficial siderosis in cerebral amyloid angiopathy. Neurology. 2019;92:e792–801.
26. Cheng AL, Batool S, McCreary CR, Lauzon ML, Frayne R, Goyal M, Smith EE. Susceptibility-weighted imaging is more reliable than T2*-weighted gradient-recalled echo MRI for detecting microbleeds. Stroke. 2013;44:2782–6.
27. Haller S, Vernooij MW, Kuijer JPA, Larsson EM, Jäger HR, Barkhof F. Cerebral microbleeds: imaging and clinical significance. Radiology. 2018;287:11–28.
28. Barakos J, Sperling R, Salloway S, Jack C, Gass A, Fiebach JB, Tampieri D, Melançon D, Miaux Y, Rippon G, Black R, Lu Y, Brashear HR, Arrighi HM, Morris KA, Grundman M. MR imaging features of amyloid-related imaging abnormalities. AJNR Am J Neuroradiol. 2013;34:1958–65.
29. Stehling C, Wersching H, Kloska SP, Kirchhof P, Ring J, Nassenstein I, Allkemper T, Knecht S, Bachmann R, Heindel W. Detection of asymptomatic cerebral microbleeds: a comparative study at 1.5 and 3.0 T. Acad Radiol. 2008;15:895–900.
30. Mittal S, Wu Z, Neelavalli J, Haacke EM. Susceptibility-weighted imaging: technical aspects and clinical applications, part 2. AJNR Am J Neuroradiol. 2009;30:232–52.
31. Wu Z, Mittal S, Kish K, Yu Y, Hu J, Haacke EM. Identification of calcification with MRI using susceptibility-weighted imaging: a case study. J Magn Reson Imaging. 2009;29:177–82.
32. Beck J, Ulrich CT, Fung C, Fichtner J, Seidel K, Fiechter M, Hsieh K, Murek M, Bervini D, Meier N, Mono ML, Mordasini P, Hewer E, Z'Graggen WJ, Gralla J, Raabe A. Diskogenic microspurs as a major cause of intractable spontaneous intracranial hypotension. Neurology. 2016;87:1220–6.
33. Schievink WI, Meyer FB, Atkinson JL, Mokri B. Spontaneous spinal cerebrospinal fluid leaks and intracranial hypotension. J Neurosurg. 1996;84:598–605.
34. Schievink WI. Spontaneous spinal cerebrospinal fluid leaks and intracranial hypotension. JAMA. 2006;295:2286–95.

35. Hosokawa M, Murata KY, Hironishi M, Koh J, Nishioka K, Nakao N, Ito H. Superficial siderosis associated with duplicated dura mater detected by CISS reverse MRI. J Neurol Sci. 2018;392:38–43.
36. Hoxworth JM, Patel AC, Bosch EP, Nelson KD. Localization of a rapid CSF leak with digital subtraction myelography. AJNR Am J Neuroradiol. 2009;30:516–9.
37. Kumar N, Lindell EP, Wilden JA, Davis DH. Role of dynamic CT myelography in identifying the etiology of superficial siderosis. Neurology. 2005;65:486–8.
38. Ellika S, Marin H, Pace M, Newman D, Abdulhak M, Kole M. Case Series: Long segment extra-arachnoid fluid collections: Role of dynamic CT myelography in diagnosis and treatment planning. Indian J Radiol Imaging. 2012;22:108–15.
39. Nose Y, Uwano I, Tateishi U, Sasaki M, Yokota T, Sanjo N. Quantitative clinical and radiological recovery in post-operative patients with superficial siderosis by an iron chelator. J Neurol. 2022;269:2539–48.
40. Arrighi HM, Barakos J, Barkhof F, Tampieri D, Jack C Jr, Melançon D, Morris K, Ketter N, Liu E, Brashear HR. Amyloid-related imaging abnormalities-haemosiderin (ARIA-H) in patients with Alzheimer's disease treated with bapineuzumab: a historical, prospective secondary analysis. J Neurol Neurosurg Psychiatry. 2016;87:106–12.
41. Linn J, Michl S, Katja B, Pfefferkorn T, Wiesmann M, Hartz S, Dichgans M, Brückmann H. Cortical vein thrombosis: the diagnostic value of different imaging modalities. Neuroradiology. 2010;52:899–911.
42. Linn J, Brückmann H. Cerebral venous and dural sinus thrombosis: state-of-the-art imaging. Clin Neuroradiol. 2010;20:25–37.
43. Scolding NJ. Central nervous system vasculitis. Semin Immunopathol. 2009;31:527–36.
44. Jennette JC, Falk RJ. Small-vessel vasculitis. N Engl J Med. 1997;337:1512–23.
45. Jennette JC, Falk RJ, Bacon PA, Basu N, Cid MC, Ferrario F, Flores-Suarez LF, Gross WL, Guillevin L, Hagen EC, Hoffman GS, Jayne DR, Kallenberg CG, Lamprecht P, Langford CA, Luqmani RA, Mahr AD, Matteson EL, Merkel PA, Ozen S, Pusey CD, Rasmussen N, Rees AJ, Scott DG, Specks U, Stone JH, Takahashi K, Watts RA. 2012 revised International Chapel Hill Consensus Conference Nomenclature of Vasculitides. Arthritis Rheum. 2013;65:1–11.
46. Berlit P. Diagnosis and treatment of cerebral vasculitis. Ther Adv Neurol Disord. 2010;3:29–42.
47. Birnbaum J, Hellmann DB. Primary angiitis of the central nervous system. Arch Neurol. 2009;66:704–9.
48. Barkhof F, Daams M, Scheltens P, Brashear HR, Arrighi HM, Bechten A, Morris K, McGovern M, Wattjes MP. An MRI rating scale for amyloid-related imaging abnormalities with edema or effusion. AJNR Am J Neuroradiol. 2013;34:1550–5.
49. Carlson C, Siemers E, Hake A, Case M, Hayduk R, Suhy J, Oh J, Barakos J. Amyloid-related imaging abnormalities from trials of solanezumab for Alzheimer's disease. Alzheimers Dement (Amst). 2016;2:75–85.
50. Iliff JJ, Wang M, Liao Y, Plogg BA, Peng W, Gundersen GA, Benveniste H, Vates GE, Deane R, Goldman SA, Nagelhus EA, Nedergaard M. A paravascular pathway facilitates CSF flow through the brain parenchyma and the clearance of interstitial solutes, including amyloid β. Sci Transl Med. 2012;4:147ra111.
51. Attems J, Yamaguchi H, Saido TC, Thal DR. Capillary CAA and perivascular Aβ-deposition: two distinct features of Alzheimer's disease pathology. J Neurol Sci. 2010;299:155–62.
52. Kress BT, Iliff JJ, Xia M, Wang M, Wei HS, Zeppenfeld D, Xie L, Kang H, Xu Q, Liew JA, Plog BA, Ding F, Deane R, Nedergaard M. Impairment of paravascular clearance pathways in the aging brain. Ann Neurol. 2014;76:845–61.
53. Weller RO, Subash M, Preston SD, Mazanti I, Carare RO. Perivascular drainage of Amyloid-b Peptides from the brain and its failure in cerebral Amyloid angiopathy and Alzheimer's disease. Brain Pathol. 2008;18:253–66.
54. Weller RO, Hawkes CA, Kalaria RN, Werring DJ, Carare RO. White matter changes in dementia: role of impaired drainage of interstitial fluid. Brain Pathol. 2015;25:63–78.
55. Carare RO, Hawkes CA, Jeffrey M, Kalaria RN, Weller RO. Review: cerebral amyloid angiopathy, prion angiopathy, CADASIL and the spectrum of protein elimination failure angiopathies (PEFA) in neurodegenerative disease with a focus on therapy. Neuropathol Appl Neurobiol. 2013;39:593–611.
56. Benveniste H, Liu X, Koundal S, Sanggaard S, Lee H, Wardlaw J. The glymphatic system and waste clearance with brain aging: a review. Gerontology. 2019;65:106–19.
57. Roher AE, Kuo YM, Esh C, Knebel C, Weiss N, Kalback W, Luehrs DC, Childress JL, Beach TG, Weller RO, Kokjohn TA. Cortical and leptomeningeal cerebrovascular amyloid and white matter pathology in Alzheimer's disease. Mol Med. 2003;9:112–22.
58. Zhang ET, Inman CBE, Weller RO. Interrelationships of the pia mater and the perivascular (Virchow-Robin) spaces in the human cerebrum. J Anat. 1990;170:111–23.
59. Brenowitz WD, Nelson PT, Besser LM, Heller KB, Kukull WA. Cerebral amyloid angiopathy and its co-occurrence with Alzheimer's disease and other cerebrovascular neuropathologic changes. Neurobiol Aging. 2015;36:2702–8.
60. Greenberg SM, Bacskai BJ, Hernandez-Guillamon M, Pruzin J, Sperling R, van Veluw SJ. Cerebral amyloid angiopathy and Alzheimer disease—one peptide, two pathways. Nat Rev Neurol. 2020;16:30–42.
61. Thal DR, Ghebremedhin E, Rüb U, Yamaguchi H, Del Tredici K, Braak H. Two types of sporadic cerebral amyloid angiopathy. J Neuropathol Exp Neurol. 2002;61:282–93.
62. Thal DR, Ghebremedhin E, Orantes M, Wiestler OD. Vascular pathology in Alzheimer disease: correlation of cerebral amyloid angiopathy and arteriosclerosis/lipohyalinosis with cognitive decline. J Neuropathol Exp Neurol. 2003;62:1287–301.
63. Thal DR, Papassotiropoulos A, Saido TC, Griffin WS, Mrak RE, Kölsch H, Del Tredici K, Attems J, Ghebremedhin E. Capillary cerebral amyloid angiopathy identifies a distinct APOE epsilon4-associated subtype of sporadic Alzheimer's disease. Acta Neuropathol. 2010;120:169–83.
64. Miller DL, Papayannopoulos IA, Styles J, Bobin SA, Lin YY, Biemann K, Iqbal K. Peptide compositions of the cerebrovascular and senile plaque core amyloid deposits of Alzheimer's disease. Arch Biochem Biophys. 1993;301:41–52.
65. Gkanatsiou E, Portelius E, Toomey CE, Blennow K, Zetterberg H, Lashley T, Brinkmalm G. A distinct brain beta amyloid signature in cerebral amyloid angiopathy compared to Alzheimer's disease. Neurosci Lett. 2019;701:125–31.
66. Jarrett JT, Berger EP, Lansbury PT. The carboxy terminus of the beta amyloid protein is critical for the seeding of amyloid formation: implications for the pathogenesis of Alzheimer's disease. Biochem. 1993;32:4693–7.
67. Charidimou A, Boulouis G, Pasi M, Auriel E, van Etten ES, Haley K, Ayres A, Schwab KM, Martinez-Ramirez S, Goldstein JN, Rosand J, Viswanathan A, Greenberg SM, Gurol ME. MRI-visible perivascular spaces in cerebral amyloid angiopathy and hypertensive arteriopathy. Neurology. 2017;88:1157–64.
68. Ding J, Sigurðsson S, Jónsson PV, Eiriksdottir G, Charidimou A, Lopez OL, van Buchem MA, Guðnason V, Launer LJ. Large Perivascular Spaces Visible on Magnetic Resonance Imaging, Cerebral Small Vessel Disease Progression, and Risk of Dementia: The Age, Gene/Environment Susceptibility-Reykjavik Study. JAMA Neurol. 2017;74:1105–12.

69. Greenberg SM, Charidimou A. Diagnosis of cerebral amyloid angiopathy: evolution of the Boston criteria. Stroke. 2018;49:491–7.
70. Greenberg SM, Vernooij MW, Cordonnier C, Viswanathan A, Al-Shahi Salman R, Warach S, Launer LJ, Van Buchem MA, Breteler MM; Microbleed Study Group. Cerebral microbleeds: a guide to detection and interpretation. Lancet Neurol. 2009;8:165–74.
71. Pantoni L. Cerebral small vessel disease: from pathogenesis and clinical characteristics to therapeutic challenges. Lancet Neurol. 2010;9:689–701.
72. Wardlaw JM, Smith EE, Biessels GJ, Cordonnier C, Fazekas F, Frayne R, Lindley RI, O'Brien JT, Barkhof F, Benavente OR, Black SE, Brayne C, Breteler M, Chabriat H, Decarli C, de Leeuw FE, Doubal F, Duering M, Fox NC, Greenberg S, Hachinski V, Kilimann I, Mok V, Oostenbrugge Rv, Pantoni L, Speck O, Stephan BC, Teipel S, Viswanathan A, Werring D, Chen C, Smith C, van Buchem M, Norrving B, Gorelick PB, Dichgans M; STandards for ReportIng Vascular changes on nEuroimaging (STRIVE v1). Neuroimaging standards for research into small vessel disease and its contribution to ageing and neurodegeneration. Lancet Neurol. 2013;12:822–38.
73. Nichtweiß M, Weidauer S, Treusch N, Hattingen E. White matter lesions and vascular cognitive impairment. Part 1: typical and unusual causes. Clin Neuroradiol. 2012;22:193–210.
74. Wardlaw J, Smith C, Dichgans M. Mechanisms underlying sporadic cerebral small vessel disease: insights from neuroimaging. Lancet Neurol. 2013;12:483–97.
75. Duering M, Csanadi E, Gesierich B, Jouvent E, Hervé D, Seiler S, Belaroussi B, Ropele S, Schmidt R, Chabriat H, Dichgans M. Incident lacunes preferentially localize to the edge of white matter hyperintensities: insights into the pathophysiology of cerebral small vessel disease. Brain. 2013;136:2717–26.
76. Pantoni L, Basile AM, Pracucci G, Asplund K, Bogousslavsky J, Chabriat H, Erkinjuntti T, Fazekas F, Ferro JM, Hennerici M, O'brien J, Scheltens P, Visser MC, Wahlund LO, Waldemar G, Wallin A, Inzitari D. Impact of age-related cerebral white matter changes on the transition to disability -- the LADIS study: rationale, design and methodology. Neuroepidemiology. 2005;24:51–62.
77. Charidimou A, Boulouis G, Haley K, Auriel E, van Etten ES, Fotiadis P, Reijmer Y, Ayres A, Vashkevich A, Dipucchio ZY, Schwab KM, Martinez-Ramirez S, Rosand J, Viswanathan A, Greenberg SM, Gurol ME. White matter hyperintensity patterns in cerebral amyloid angiopathy and hypertensive arteriopathy. Neurology. 2016;86:505–11.
78. Purrucker JC, Steiner T. Atypical intracerebral hemorrhage—etiology and acute management. Nervenarzt. 2019;90:423–41.
79. Charidimou A, Shakeshaft C, Werring DJ. Cerebral microbleeds on magnetic resonance imaging and anticoagulant-associated intracerebral hemorrhage risk. Front Neurol. 2012;3:133.
80. Greenberg SM, Vonsattel JP, Stakes JW, Gruber M, Finklestein SP. The clinical spectrum of cerebral amyloid angiopathy: presentations without lobar hemorrhage. Neurology. 1993;43:2073–9.
81. Salloway S, Chalkias S, Barkhof F, Burkett P, Barakos J, Purcell D, Suhy J, Forrestal F, Tian Y, Umans K, Wang G, Singhal P, Budd Haeberlein S, Smirnakis K. Amyloid-Related Imaging Abnormalities in 2 Phase 3 Studies Evaluating Aducanumab in Patients With Early Alzheimer Disease. JAMA Neurol. 2022;79:13–21.
82. VandeVrede L, Gibbs DM, Koestler M, La Joie R, Ljubenkov PA, Provost K, Soleimani-Meigooni D, Strom A, Tsoy E, Rabinovici GD, Boxer AL. Symptomatic amyloid-related imaging abnormalities in an APOE ε4/ε4 patient treated with aducanumab. Alzheimers Dement (Amst). 2020;12:e12101. Erratum in: Alzheimers Dement (Amst). 2020;12:e12134.
83. Sanchez-Caro JM, de Lorenzo Martínez de Ubago I, de Celis Ruiz E, Arribas AB, Calviere L, Raposo N, Blancart RG, Fuentes B, Diez-Tejedor E, Rodriguez-Pardo J. Transient Focal Neurological Events in Cerebral Amyloid Angiopathy and the Long-term Risk of Intracerebral Hemorrhage and Death: A Systematic Review and Meta-analysis. JAMA Neurol. 2022;79:38–47.
84. Marini S, Crawford K, Morotti A, Lee MJ, Pezzini A, Moomaw CJ, Flaherty ML, Montaner J, Roquer J, Jimenez-Conde J, Giralt-Steinhauer E, Elosua R, Cuadrado-Godia E, Soriano-Tarraga C, Slowik A, Jagiella JM, Pera J, Urbanik A, Pichler A, Hansen BM, McCauley JL, Tirschwell DL, Selim M, Brown DL, Silliman SL, Worrall BB, Meschia JF, Kidwell CS, Testai FD, Kittner SJ, Schmidt H, Enzinger C, Deary IJ, Rannikmae K, Samarasekera N, Al-Shahi Salman R, Sudlow CL, Klijn CJM, van Nieuwenhuizen KM, Fernandez-Cadenas I, Delgado P, Norrving B, Lindgren A, Goldstein JN, Viswanathan A, Greenberg SM, Falcone GJ, Biffi A, Langefeld CD, Woo D, Rosand J, Anderson CD; International Stroke Genetics Consortium. Association of Apolipoprotein E With Intracerebral Hemorrhage Risk by Race/Ethnicity: A Meta-analysis. JAMA Neurol. 2019;76:480–91.
85. Sakai K, Boche D, Carare R, Johnston D, Holmes C, Love S, Nicoll JA. Aβ immunotherapy for Alzheimer's disease: effects on apoE and cerebral vasculopathy. Acta Neuropathol. 2014;128:777–89.
86. Greenberg SM, Al-Shahi Salman R, Biessels GJ, van Buchem M, Cordonnier C, Lee JM, Montaner J, Schneider JA, Smith EE, Vernooij M, Werring DJ. Outcome markers for clinical trials in cerebral amyloid angiopathy. Lancet Neurol. 2014;13:419–28.
87. Kalaria RN, Ihara M. Vascular and neurodegenerative pathways—will they meet? Nat Rev Neurol. 2013;9:487–8.
88. Jack CR Jr, Knopman DS, Jagust WJ, Shaw LM, Aisen PS, Weiner MW, Petersen RC, Trojanowski JQ. Hypothetical model of dynamic biomarkers of the Alzheimer's pathological cascade. Lancet Neurol. 2010;9:119–28.
89. Corriveau RA, Bosetti F, Emr M, Gladman JT, Koenig JI, Moy CS, Pahigiannis K, Waddy SP, Koroshetz W. The Science of Vascular Contributions to Cognitive Impairment and Dementia (VCID): A Framework for Advancing Research Priorities in the Cerebrovascular Biology of Cognitive Decline. Cell Mol Neurobiol. 2016;36:281–8.
90. Frisoni GB, Galluzzi S, Pantoni L, Filippi M. The effect of white matter lesions on cognition in the elderly—small but detectable. Nat Clin Pract Neurol. 2007;3:620–7.
91. Frisoni GB. The clinical use of structural MRI in Alzheimer's disease. Nat Rev Neurol. 2010;6:67–77.
92. Goos JD, Kester MI, Barkhof F, Klein M, Blankenstein MA, Scheltens P, van der Flier WM. Patients with Alzheimer disease with multiple microbleeds: relation with cerebrospinal fluid biomarkers and cognition. Stroke. 2009;40:3455–60.
93. Caetano A, Ladeira F, Barbosa R, Calado S, Viana-Baptista M. Cerebral amyloid angiopathy—The modified Boston criteria in clinical practice. J Neurol Sci. 2018;384:55–7.
94. Smith EE, Charidimou A, Ayata C, Werring DJ, Greenberg SM. Cerebral amyloid angiopathy-related transient focal neurologic episodes. Neurology. 2021;97:231–8.
95. Charidimou A, Peeters A, Fox Z, Gregoire SM, Vandermeeren Y, Laloux P, Jäger HR, Baron JC, Werring DJ. Spectrum of transient focal neurological episodes in cerebral amyloid angiopathy: multicentre magnetic resonance imaging cohort study and meta-analysis. Stroke. 2012;43:2324–30.
96. Charidimou A. Cerebral amyloid angiopathy-related transient focal neurological episodes (CAA-TFNEs): a well-defined clinical-radiological syndrome. J Neurol Sci. 2019;406:116496.
97. Dreier JP. The role of spreading depression, spreading depolarization and spreading ischemia in neurological disease. Nat Med. 2011;17:439–47.
98. Saade C, Najem E, Asmar K, Salman R, El Achkar B, Naffaa L. Intracranial calcifications on CT: an updated review. Radiology Case. 2019;13:1–18.
99. Rasing I, Voigt S, Koemans EA, van Zwet E, de Kruijff PC, van Harten TW, van Etten ES, van Rooden S, van der Weerd L, van

Buchem MA, van Osch MJP, Greenberg SM, van Walderveen MAA, Terwindt GM, Wermer MJH. Occipital Cortical Calcifications in Cerebral Amyloid Angiopathy. Stroke. 2021;52:1851–5.
100. Maheshwari U, Huang SF, Sridhar S, Keller A. The interplay between brain vascular calcification and microglia. Front Aging Neurosci. 2022;14:Article 848495.
101. Koob M, Laugel V, Durand M, Fothergill H, Dalloz C, Sauvanaud F, Dollfus H, Namer IJ, Dietemann JL. Neuroimaging in Cockayne syndrome. AJNR Am J Neuroradiol. 2010;31:1623–30.
102. Cannella R, Sparacia G, Re LV, Oddo E, Mamone G, Miaglia R. Advanced magnetic resonance imaging of cortical laminar necrosis in patients with stroke. Neuroradiol J. 2019;32:431–7.
103. Bornemann KD, Wiederhold KH, Pauli C, Ermini F, Stalder M, Schnell L, Sommer B, Jucker M, Staufenbiel M. Abeta-induced inflammatory processes in microglia cells of APP23 transgenic mice. Am J Pathol. 2001;158:63–73.
104. Auriel E, Charidimou A, Gurol ME, Ni J, Van Etten ES, Martinez-Ramirez S, Boulouis G, Piazza F, DiFrancesco JC, Frosch MP, Pontes-Neto OV, Shoamanesh A, Reijmer Y, Vashkevich A, Ayres AM, Schwab KM, Viswanathan A, Greenberg SM. Validation of Clinicoradiological Criteria for the Diagnosis of Cerebral Amyloid Angiopathy-Related Inflammation. JAMA Neurol. 2016;73:197–202.
105. Antolini L, DiFrancesco JC, Zedde M, Basso G, Arighi A, Shima A, Cagnin A, Caulo M, Carare RO, Charidimou A, Cirillo M, Di Lazzaro V, Ferrarese C, Giossi A, Inzitari D, Marcon M, Marconi R, Ihara M, Nitrini R, Orlandi B, Padovani A, Pascarella R, Perini F, Perini G, Sessa M, Scarpini E, Tagliavini F, Valenti R, Vázquez-Costa JF, Villarejo-Galende A, Hagiwara Y, Ziliotto N, Piazza F. Spontaneous ARIA-like Events in Cerebral Amyloid Angiopathy-Related Inflammation: A Multicenter Prospective Longitudinal Cohort Study. Neurology. 2021;97:e1809–22.
106. Piazza F, Greenberg SM, Savoiardo M, Gardinetti M, Chiapparini L, Raicher I, Nitrini R, Sakaguchi H, Brioschi M, Billo G, Colombo A, Lanzani F, Piscosquito G, Carriero MR, Giaccone G, Tagliavini F, Ferrarese C, DiFrancesco JC. Anti-amyloid β autoantibodies in cerebral amyloid angiopathy-related inflammation: implications for amyloid-modifying therapies. Ann Neurol. 2013;73:449–58.
107. Sperling RA, Jack CR Jr, Black SE, Frosch MP, Greenberg SM, Hyman BT, Scheltens P, Carrillo MC, Thies W, Bednar MM, Black RS, Brashear HR, Grundman M, Siemers ER, Feldman HH, Schindler RJ. Amyloid-related imaging abnormalities in amyloid-modifying therapeutic trials: recommendations from the Alzheimer's Association Research Roundtable Workgroup. Alzheimers Dement. 2011;7:367–85.
108. Sperling R, Salloway S, Brooks DJ, Tampieri D, Barakos J, Fox NC, Raskind M, Sabbagh M, Honig LS, Porsteinsson AP, Lieberburg I, Arrighi HM, Morris KA, Lu Y, Liu E, Gregg KM, Brashear HR, Kinney GG, Black R, Grundman M. Amyloid-related imaging abnormalities in patients with Alzheimer's disease treated with bapineuzumab: a retrospective analysis. Lancet Neurol. 2012;11:241–9.
109. Eng JA, Frosch MP, Choi K, Rebeck GW, Greenberg SM. Clinical manifestations of cerebral amyloid angiopathy-related inflammation. Ann Neurol. 2004;55:250–6.
110. Coulette S, Renard D, Lehmann S, Raposo N, Arquizan C, Charif M, Thouvenot E, Wacongne A, Viguier A, Bonneville F, Allou T, Boukriche Y, Chiper L, Blanchet Fourcade G, Gabelle A, Ducros A, Duflos C, Labauge P, Menjot de Champfleur N, Ayrignac X. A Clinico-Radiological Study of Cerebral Amyloid Angiopathy-Related Inflammation. Cerebrovasc Dis. 2019;48:38–44.
111. Kinnecom C, Lev MH, Wendell L, Smith EE, Rosand J, Frosch MP, Greenberg SM. Course of cerebral amyloid angiopathy-related inflammation. Neurology. 2007;68:1411–6.
112. Regenhardt RW, Thon JM, Das AS, Thon OR, Charidimou A, Viswanathan A, Gurol ME, Chwalisz BK, Frosch MP, Cho TA, Greenberg SM. Association Between Immunosuppressive Treatment and Outcomes of Cerebral Amyloid Angiopathy-Related Inflammation. JAMA Neurol. 2020;77:1261–9.
113. Scolding NJ, Joseph F, Kirby PA, Mazanti I, Gray F, Mikol J, Ellison D, Hilton DA, Williams TL, MacKenzie JM, Xuereb JH, Love S. Abeta-related angiitis: primary angiitis of the central nervous system associated with cerebral amyloid angiopathy. Brain. 2005;128:500–15.
114. Salvarani C, Hunder GG, Morris JM, Brown RD Jr, Christianson T, Giannini C. Aβ-related angiitis comparison with CAA without inflammation and primary CNS vasculitis. Neurology. 2013;81:1596–603.
115. Chung KK, Anderson NE, Hutchinson D, Synek B, Barber PA. Cerebral amyloid angiopathy related inflammation: three case reports and a review. J Neurol Neurosurg Psychiatr. 2011;82:20–6.
116. Schaumberg J, Trauscheid M, Eckert B, Petersen D, Schulz-Schaeffer W, Röther J, Heide W. Zerebrale Amyloidangiopathie assoziiert mit Inflammation [Cerebral amyloid angiopathy associated with inflammation]. Nervenarzt. 2018;89:682–91.
117. Traschütz A, Tzaridis T, Penner AH, Kuchelmeister K, Urbach H, Hattingen E, Heneka MT. Reduction of microbleeds by immunosuppression in a patient with Aβ-related vascular inflammation. Neurol Neuroimmunol Neuroinflamm. 2015;2:e165.
118. Wengert O, Harms L, Siebert E. Cerebral amyloid angiopathy-related inflammation: a treatable cause of rapidly-progressive dementia. J Neuropsychiatry Clin Neurosci. 2012;24:E1–E2.
119. Sevigny J, Chiao P, Bussière T, Weinreb PH, Williams L, Maier M, Dunstan R, Salloway S, Chen T, Ling Y, O'Gorman J, Qian F, Arastu M, Li M, Chollate S, Brennan MS, Quintero-Monzon O, Scannevin RH, Arnold HM, Engber T, Rhodes K, Ferrero J, Hang Y, Mikulskis A, Grimm J, Hock C, Nitsch RM, Sandrock A. The antibody aducanumab reduces Aβ plaques in Alzheimer's disease. Nature. 2016;537:50–6. Update in: Nature. 2017;546:564.
120. Cummings J, Lee G, Ritter A, Sabbagh M, Zhong K. Alzheimer's disease drug development pipeline: 2020. Alzheimers Dement. 2020;6:1–29.